





HLA-DR–Expressing Fibroblast-Like Synoviocytes Are Inducible Antigen Presenting Cells That Present Autoantigens in Lyme Arthritis

Joseph R. Rouse,¹  Rebecca Danner,¹ Amanda Wahhab,¹ Michaela Pereckas,¹ Christine Nguyen,¹ Mecailla E. McClune,²  Allen C. Steere,³  Klemen Strle,⁴ Brandon L. Jutras,² and Robert B. Lochhead¹ 

Objective. HLA-DR–expressing fibroblast-like synoviocytes (FLS) are a prominent cell type in synovial tissue in chronic inflammatory forms of arthritis. FLS-derived extracellular matrix (ECM) proteins, including fibronectin-1 (FN1), contain immunogenic CD4+ T cell epitopes in patients with postinfectious Lyme arthritis (LA). However, the role of FLS in presentation of these T cell epitopes remains uncertain.

Methods. Primary LA FLS and primary murine FLS stimulated with interferon gamma (IFN γ), *Borrelia burgdorferi*, and/or *B burgdorferi* peptidoglycan (PG) were assessed for properties associated with antigen presentation. HLA-DR–presented peptides from stimulated LA FLS were identified by immunopeptidomics analysis. OT-II T cells were co-cultured with stimulated murine FLS in the presence of cognate ovalbumin antigen to determine the potential of FLS to act as inducible antigen presenting cells (APCs).

Results. FLS expressed HLA-DR molecules within inflamed synovial tissue and tendons from patients with postinfectious LA in situ. Major histocompatibility complex (MHC) class II and co-stimulatory molecules were expressed by FLS following in vitro stimulation with IFN γ and *B burgdorferi* and presented both foreign and self-MHC-II peptides, including an immunogenic T cell epitope derived from Lyme autoantigen FN1. Stimulated FLS induced proliferation of naive OT-II CD4+ T cells that were dependent on OT-II antigen and CD40. Stimulation with *B burgdorferi* PG enhanced FLS-mediated T cell activation.

Conclusion. MHC-II+ FLS are inducible APCs that can induce CD4+ T cell activation in an antigen- and CD40-dependent manner. Activated FLS can also present ECM-derived Lyme autoantigens, implicating FLS in amplifying tissue-localized autoimmunity in LA.

INTRODUCTION

HLA-DR–expressing fibroblast-like synoviocytes (FLS) are believed to be key drivers of synovial inflammation.^{1–4} We have recently demonstrated that synovial extracellular matrix (ECM) proteins, including fibronectin-1 (FN1), are targets of autoimmune CD4+ T cell responses in over half of patients with postinfectious Lyme arthritis (LA), defined as patients who fail to fully resolve their arthritis after two to three months of appropriate antibiotic therapy

and apparent killing of the Lyme disease spirochete *Borrelia burgdorferi*. FLS are major producers of ECM proteins, and HLA-DR+ FLS are highly abundant in postinfectious LA synovial tissue,⁵ and we have hypothesized that FLS are both producing and presenting Lyme autoantigens.^{1,2} However, this hypothesis has not yet been fully tested.

FLS are synovial tissue resident cells that are important in joint health and disease. FLS are (1) the primary cell type within joint synovial tissue, (2) responsible for production and

Opinions, interpretations, conclusions, and recommendations are those of the authors and are not necessarily endorsed by the NIH or the Department of Defense.

Drs Jutras and Lochhead were supported by the NIH (grants 1R21-AI-148982-01, 1R01-AI-173256-01, and 1R01-AI-178711-01) and by the Assistant Secretary of Defense for Health Affairs through the Tick-Borne Disease Research Program, endorsed by the Department of Defense (grant W81XWH-22-1-0728).

¹Joseph R. Rouse, Rebecca Danner, Amanda Wahhab, Michaela Pereckas, Christine Nguyen, Robert B. Lochhead, PhD: Medical College of Wisconsin, Milwaukee; ²Mecailla E. McClune, Brandon L. Jutras: Virginia Polytechnic Institute and State University, Blacksburg; ³Allen C. Steere: Massachusetts

General Hospital and Harvard Medical School, Boston; ⁴Klemen Strle: Tufts University, Boston, Massachusetts.

Additional supplementary information cited in this article can be found online in the Supporting Information section (<https://acrjournals.onlinelibrary.wiley.com/doi/10.1002/acr2.11710>).

Author disclosures are available at <https://onlinelibrary.wiley.com/doi/10.1002/acr2.11710>.

Address correspondence via email to Robert B Lochhead, PhD, at rlochhead@mcw.edu

Submitted for publication May 16, 2024; accepted in revised form June 10, 2024.

maintenance of the ECM, (3) critical for tissue repair, and (4) required to achieve homeostasis following an inflammatory insult.⁶ Under chronic inflammatory conditions, however, FLS play a critical role in driving pathogenesis. In rheumatoid arthritis (RA), the prototypic autoimmune joint disease, activated HLA-DR+ FLS accumulate within the synovial lining and sublining, where they interact with CD4+ T cells and other immune cells.^{7–11} Furthermore, abundance of activated HLA-DR+ FLS positively correlates with RA disease activity.¹²

Lyme disease (LD) is caused by the tick-borne spirochete *Borrelia burgdorferi* and occurs primarily in temperate zones of North America, Europe, and Asia. Each year, an estimated 500,000 new cases occur in the United States, and the infection is epidemic in affected regions.^{13,14} LA is the most common late-stage LD manifestation in the United States and is usually effectively treated with one to three months of oral and, if necessary, IV, antibiotic therapy, called antibiotic-responsive LA.¹⁵ However, in a subset (approximately 5%) of patients, arthritis can persist or worsen, even after apparent spirochetal killing by appropriate antibiotic therapy, called postinfectious LA.¹⁵ Postinfectious LA is characterized by severe synovial hyperplasia and accumulation of large numbers of HLA-DR+ FLS within inflamed joints^{2,5,16–18} and is frequently accompanied by autoimmune T and B cell responses targeting self-proteins associated with vascular inflammation and ECM damage.^{1,2,15,19–22} In addition, peptidoglycan (PG), a pathogen-associated molecular pattern (PAMP) that is an essential cell wall component in most bacteria required for protection from osmotic pressure, is a key *B burgdorferi* antigen that can persist in joints of patients with postinfectious LA for up to several years following oral and/or IV antibiotic therapy. This spirochetal remnant may contribute to persistent arthritis after the infection itself is cleared.^{23,24}

Bacterial PG has also been detected in the inflamed synovium of patients with RA²⁵ and osteoarthritis (OA),²⁶ suggesting that PG accumulates in synovial tissue, particularly within the context of joint inflammation following an infection, such as in postinfectious LA. Moreover, PG has been reported to have an immune adjuvant effect on FLS.^{27,28} In this study, we demonstrate that HLA-DR+ FLS can present major histocompatibility complex (MHC) class II (MHC-II) epitopes, including a Lyme autoantigen derived from the ECM protein FN1, and that primary murine FLS stimulated with interferon gamma (IFN γ) and *B burgdorferi* PG can induce proliferation and activation of CD4+ T cells in an antigen-dependent manner.

MATERIALS AND METHODS

Patients and ethics. All patients with LD met the Centers for Disease Control and Prevention criteria for *B burgdorferi* infection.²⁹ All patients had swollen knees and high IgG antibody responses to *B burgdorferi*, as determined by enzyme-linked immunosorbent assay and Western blot. Patients with LA

received treatment according to an algorithm,¹⁵ as mentioned in the guidelines of the Infectious Diseases Society of America.³⁰

Mice were housed in the Medical College of Wisconsin Biomedical Resource Center, following strict adherence to the guidelines according to the National Institutes of Health for the care and use of laboratory animals, as described in the *Guide for the Care and Use of Laboratory Animals, 8th Edition*. Protocols conducted in this study were approved and carried out in accordance with the Medical College of Wisconsin Institutional Animal Care and Use Committee (protocol number AUA00006528). Mouse experiments were performed under isoflurane anesthesia, and every effort was made to minimize suffering.

The study “Immunity in Lyme Arthritis” was approved by the Human Investigations Committee at Massachusetts General Hospital, according to principles for medical research involving human participants expressed in the World Medical Association Declaration of Helsinki. Written informed consent was obtained from all participants 18 years of age or older, or from patient and a parent or guardian of those between the ages of 12 and 17 years old.

Human LA FLS analysis and liquid chromatography mass spectrometry/mass spectrometry. Human LA tissue biopsies and FLS were analyzed as described⁵ and as detailed in the Supplemental Methods. HLA-DR peptide isolation was performed as described,³¹ with modifications detailed in the Supplemental Methods. Mass spectrometry (MS) data were analyzed using Proteome Discoverer 2.4 (Thermo) platform. SequestHT was used as a search algorithm. Fixed Value (FV) and Target Decoy (TD) peptide-spectrum match (PSM) validators and Protein false discovery rate (FDR) validator were used to identify potential PSM–peptide matches. For FV validation, PSMs with cross-correlation scores (Xcorr) lower than 2.5 were excluded as potential matches. Proteome databases searched for this study were *Borrelia burgdorferi* (N40 and B31) and Human (Swissprot, with isoforms).

Bacteria and mouse strains. Mouse strains C57BL/6J (B6) and B6.Cg-Tg(TcraTcrb)425Cbn/J (OT-II) were acquired from Jackson Laboratory. The class II MHC transactivator (CIITA) enhanced green fluorescent protein (EGFP)–reporter mouse was generated as described³² and back-crossed onto the C57BL/6J background for seven generations. For the in vitro stimulation experiments using live bacteria, we used *B burgdorferi* strain B31-A3.

Primary cell stimulation and analysis. Bone marrow–derived macrophages (BMDMs) and murine FLS were isolated from bone marrow and ankle joints as described.³³ FLS were passaged at least three times to remove contaminating cells with 10% Dulbecco’s modified Eagle’s medium (DMEM). Cells were stimulated for 48 hours with IFN γ (20 ng/mL), *B burgdorferi*

(1×10^6 cells/mL), *B burgdorferi* PG (10 $\mu\text{g/mL}$). *B burgdorferi* PG was purified as previously described.³⁴ Cells and secreted cytokines were analyzed by flow cytometry, as recommended by the manufacturer (Biolegend). For a complete list of commercial antibodies and reagents used, see Supplemental Methods.

IncuCyte imaging of CIITA EGFP-reporter FLS. CIITA EGFP-reporter FLS (passage 4), were stimulated with 0, 0.2, 2, or 20 ng/mL IFN γ and compared to non-green fluorescent protein (GFP)-tagged controls. Cells were plated at 70,000 cells per well in 100 μL of medium in a 96-well plate and were allowed to rest overnight in a 32°C incubator with 5% CO $_2$. Green fluorescence (ex:440-480 nm, em:504-544 nm) was used to detect the EGFP reporter and analyzed by IncuCyte imaging with images taken every two hours for 96 hours total at 10 \times objective. Statistical analysis was performed using Tukey's multiple comparisons test ($P < 0.05$). Error bars represent SD.

T cell proliferation assay. FLS were thawed from frozen stock (passage 4) and cultured to passage 5 before plating in 24-well plates (1×10^5 cells/well) for 24 hours before stimulation. Cells were then stimulated for 48 hours with IFN γ (20 ng/mL), *B burgdorferi* PG (10 $\mu\text{g/mL}$), or both in 2% DMEM at 37°C. CD3+ T cells were isolated from spleens of six- to eight-week-old OT-II mice by MojoSort mouse CD3+ T cell isolation kit (Biolegend 480024) and stained using the Cell-Trace CFSE cell proliferation kit (ThermoFisher C34554) according to manufacturer's instructions. Stimulated FLS were washed with phosphate buffered saline (PBS) and co-cultured with CD3+ T cells at a concentration of 5 to 10×10^5 cells/mL in 10% RPMI for five days with either the cognate ovalbumin (OVA)₃₂₃₋₃₃₉ antigen (2 $\mu\text{g/mL}$, a nonreactive OVA₂₅₇₋₂₆₄ peptide (2 $\mu\text{g/mL}$), or OVA (10 $\mu\text{g/mL}$). Interleukin (IL)-2 (0.5 $\mu\text{g}/10^5$ cells) was used to maintain T cell viability. Cells were incubated with fluorochrome-coupled antibodies at manufacturer's recommended concentrations against I-ab (BioLegend #116418), CD90.2 (BioLegend #140324), CD54 (BioLegend #116141), CD3 (BioLegend #100216), CD4 (BioLegend #100412), and CD8 (BioLegend #100725). Cells were analyzed using fluorescence-activated cell sorting Celesta (Beckman Coulter) and FlowJo version 10.7.1 software. Cell-free supernatants were collected, and cytokine secretion was assayed by LegendPlex Mouse inflammation Panel (BioLegend #740446) multiplex analysis and according to the manufacturers' instructions using the Celesta Flow cytometer (Beckman Coulter) and analyzed with LegendPlex online software.

Single-cell RNA sequencing. Cells were barcoded using Parse Biosciences WTseq Minikit version 3 (ECWT3100) according to manufacturer's instructions, and libraries were sequenced on Illumina NextSeq500. Raw sequencing data were demultiplexed using Illumina bcl2fastq and converted to gene-barcode

matrixes using Parse Biosciences Pipeline. Analysis was performed in R version 4.3.1 using the package Seurat version 5. The number of genes detected per cell, number of unique molecular identifiers, and percentage of mitochondrial genes were plotted, and outliers were removed to filter dead cells.

Antibody blocking assay. FLS were thawed from frozen stock and cultured to passage 5 before plating in 24-well cell culture plates (1×10^5 cells/well) for 24 hours before stimulation. Cells were then stimulated for 48 hours with IFN γ (20 ng/mL) or IFN γ + *B burgdorferi* PG (10 $\mu\text{g/mL}$) in 2% DMEM at 37°C. Anti-I-ab antibody (Biolegend 107601), anti-CD40 antibody (Biolegend 102901), or isotype controls (Biolegend 400501 and 401002, respectively) at a concentration of 8 $\mu\text{g/mL}$. CD3+ T cells were isolated from spleens of six- to eight-week-old OT-II mice by MojoSort mouse CD3+ T cell isolation kit (Biolegend 480024). Stimulated FLS were washed with PBS before addition of blocking antibodies and CD3+ T cells at a concentration of 5 to 10×10^5 cells/mL in 10% RPMI for five days with OVA₃₂₃₋₃₃₉ antigen (2 $\mu\text{g/mL}$). IL-2 (0.5 $\mu\text{g}/10^5$ cells) was added to maintain T cell viability.

Statistical analysis. Statistically significant differences between groups were determined by one-way analysis of variance and Tukey's multiple comparisons using GraphPad Prism (version 9). For gene expression analysis, copies per million reads (CPMR) was used to normalize gene expression.

RESULTS

HLA-DR expressed by human LA FLS within synovial tissue and inflamed tendons. Synovial hyperplasia and accumulation of activated FLS expressing HLA-DR MHC-II molecules are hallmarks of human postinfectious LA.^{2,5} We examined HLA-DR expression of vimentin+ stromal cells in synovial tissue and tendon biopsies from patients with postinfectious LA (Figure 1A). HLA-DR+/vimentin+ double-positive stromal cells (eg, HLA-DR+ FLS) were primarily localized within the synovial sublining (Figure 1A, patients 1 and 2), consistent with a similar study examining a larger number of synovial tissue biopsies.⁵ In two patients with postinfectious LA with tenosynovitis for which tendons were available, double-positive cells were also observed primarily along the lining of inflamed joint tendons (Figure 1A, patients 3 and 4). This would mark the first report, to our knowledge, of HLA-DR+ stromal cells observed in the tendons of patients with postinfectious LA, which is consistent with reports of ligamentous tissue as a reservoir of *B burgdorferi* during chronic Lyme borreliosis³⁵ and significant tendinopathy seen in LA during active infection³⁶ and in postinfectious LA.³⁷

HLA-DR expressed by human LA FLS express genes associated with antigen presentation when stimulated with IFN γ . FLS do not express the canonical B7 co-stimulatory

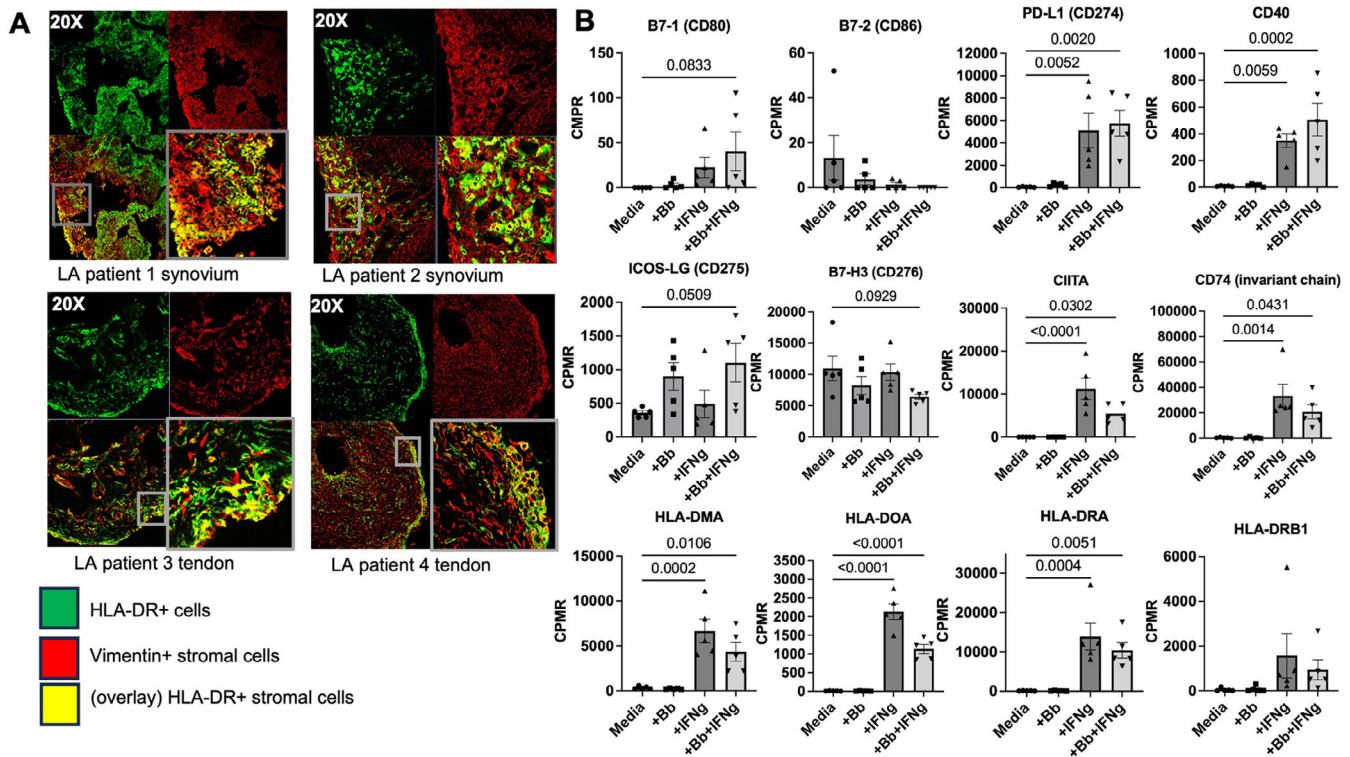


Figure 1. FLS expression of MHC class II and co-stimulatory molecules is induced by IFN γ . (A) Characterization of synovial and tendon tissue samples from four different patients with LA. Representative images of co-localization of HLA-DR and vimentin in two LA synovial and two tendon tissue biopsies. (B) Bulk RNA sequencing analysis of one patients with LA's (patient 1) FLS stimulated ex vivo with IFN γ , *Borrelia burgdorferi* (Bb), or both. Statistical analysis was performed using Tukey's multiple comparisons test (*P* values indicated in figure). Error bars represent standard errors from mean. CPMR, copies per million reads; FLS, fibroblast-like synoviocytes; IFN γ , interferon gamma; LA, interferon gamma; MHC, major histocompatibility complex; PD, programmed death.

molecules B7-1 (CD80) or B7-2 (CD86), although FLS express other B7 family co-stimulatory molecules that may play a role in antigen presentation.³⁸ We examined expression of potential co-stimulatory molecules using a human LA FLS RNA sequencing (RNA-seq) dataset generated as part of an earlier study.⁵ Primary LA FLS were stimulated with either *B burgdorferi*, IFN γ , or *B burgdorferi* + IFN γ together, and expression of genes associated with antigen processing and presentation was assessed (Figure 1B). As expected, expression of co-stimulatory molecules B7-1 and B7-2 were not consistently expressed at levels above zero (Figure 1B). However, other signal two molecules were expressed by FLS. Programmed death (PD)-L1 and CD40 were both strongly up-regulated in response to IFN γ stimulation, expression of ICOS-LG trended up in response to *B burgdorferi* + IFN γ stimulation, and expression of B7-H3 trended down with *B burgdorferi* + IFN γ stimulation (Figure 1B). Expression of genes associated with regulation of the MHC-II locus (eg, CIITA), class II antigen loading (eg, CD74/invariant chain, HLA-DM, and HLA-DO), and presentation to CD4+ T cells (eg, HLA-DR) was increased in FLS stimulated with IFN γ or IFN γ + *B burgdorferi*.

Lyme autoantigens presented by human LA FLS.

Postinfectious LA is frequently accompanied by autoimmune T

and B cell reactivity against certain HLA-DR-presented self-antigens, which were previously identified in patients' synovial tissue and/or synovial fluid mononuclear cells using an unbiased immunopeptidomics approach.³⁹ A subset of these Lyme autoantigens is derived from ECM proteins, which include FN1, laminin B2, collagen V α 1, and matrix metalloprotease 10.^{1,20} Another subset is derived from proteins involved in vascular damage, which include endothelial cell growth factor (ECGF),²¹ annexin A2,²² and apolipoprotein B-100.¹⁹ We and others have previously speculated that HLA-DR+ FLS may present some of these autoantigens within inflamed synovial tissue, thereby contributing to tissue-localized CD4+ T cell autoimmunity.^{1,2,5} Furthermore, we presume that autoimmunity is initiated during infection with *B burgdorferi*.

We used an in vitro immunopeptidomics approach using primary human LA FLS to test whether activated HLA-DR+ FLS were able to present MHC-II antigens, including potential Lyme autoantigens and foreign antigens derived from *B burgdorferi*. FLS were isolated from synovial tissue collected from a patient with LA during the postinfectious period (same patient as patient 1 shown in Figure 1A), whose HLA-DRB type is HLA-DRB1*0701/DRB1*1454. Cells were passaged over six times before use to remove any potential antigens retained from

the time of initial sample collection. FLS were stimulated with IFN γ and *B burgdorferi* (10:1 multiplicity of infection [MOI]) for 48 hours, following which HLA-DR peptides were isolated, purified, and identified by liquid chromatography MS/MS (LC-MS/MS) as described³⁹ (Figure 2A).

FV validator analysis, with a minimum Xcorr of 2.5, was used to identify 695 total peptides (Supplemental Table S1), including 10 peptides derived from *B burgdorferi* proteins (Supplemental Table S2). Of the *B burgdorferi* proteins, four are predicted to be localized to the inner membrane, three are cytosolic, and two with

unknown localization or function. Three source proteins were involved in chemotaxis/motility, three in sugar transport, two in transcription and translation. Surprisingly, none of these *B burgdorferi* peptides were derived from surface lipoproteins, which are immunodominant B cell antigens.⁴⁰

We also identified 685 peptides derived from 367 unique human proteins using FV validation analysis (Supplemental Table S1). The most abundant source protein of peptides identified was the Invariant chain, suggesting FLS are engaging in endogenous formation and transport of MHC-II peptide

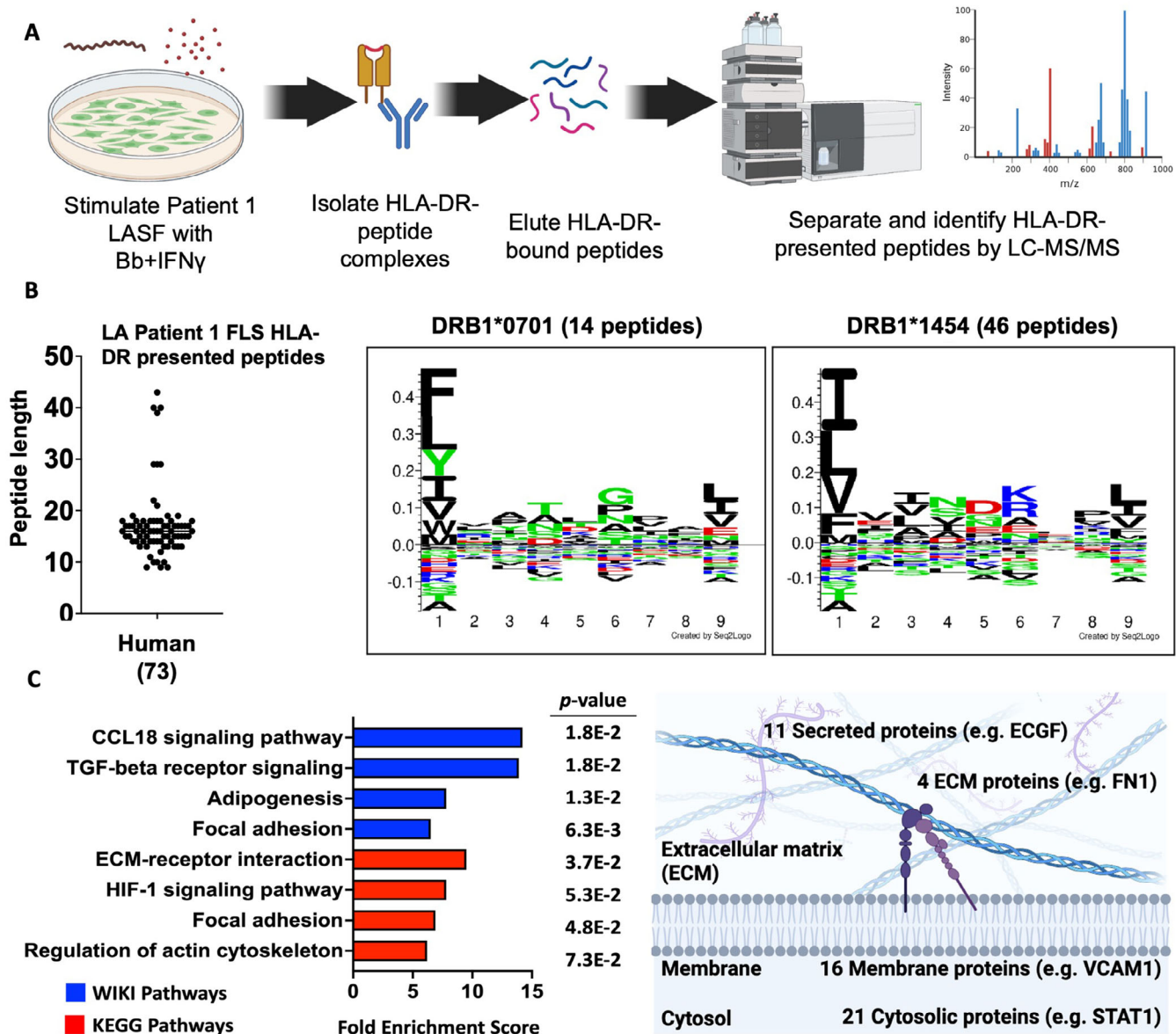


Figure 2. (A) Human LA FLS present MHC-II peptides derived from Lyme autoantigens Immunopeptidomics screen of unique LA patient FLS HLA-DR-presented peptides. (B) Peptide length and predicted HLA binding motifs of peptides predicted by both FV and TD analyses corresponding with LA patient 1 HLA-DR type. (C) WIKI Pathways, KEGG Pathways, and Gene Ontology cellular localization analyses showing enriched pathways and cellular localization associated with source proteins. ECGF, endothelial cell growth factor; FLS, fibroblast-like synoviocytes; FN1, fibronectin-1; FV, Fixed Value; IFN γ , interferon gamma; LA, Lyme arthritis; LASF, Lyme arthritis synovial fibroblasts; LC-MS/MS, liquid chromatography mass spectrometry/mass spectrometry; MHC-II, major histocompatibility complex class II; TD, Target Decoy; TGF β , tumor growth factor, beta.

complexes, and is consistent with CD74 gene expression data from Figure 1B. Proteins associated with the ECM were also abundantly represented in our dataset, with the top three KEGG Pathway functional annotation terms being (1) focal adhesion, (2) alanine, aspartate, and glutamate metabolism, and (3) ECM–receptor interactions. Interestingly, the peptide size had a binomial distribution, with 433 (63%) of the peptides >25 amino acids long (median length = 42 amino acids), and 262 (38%) of the peptides 9 to 25 amino acids long (median value = 17 amino acids), the latter being typical of fully processed MHC-II-bound peptides.⁴¹

A second, more stringent TD validation analysis was also performed, using both a 1% FDR cutoff and an Xcorr cutoff of 2.5 to minimize the potential number of false positive peptide-spectrum matches. Using this highly stringent method, we identified 73 unique predicted peptides derived from 50 human proteins (Supplemental Table S1), nearly all of which were 13 to 18 amino acids long, typical of fully processed MHC-II peptides (Figure 2B). Although all 73 peptides were also identified using FV analysis, no *B burgdorferi*-derived peptides were identified using this stringent TD analysis method. Of the 73 human peptides identified, 14 peptides were predicted to bind to the peptide binding groove of DRB1*0701, and 46 peptides were predicted to bind to the peptide binding groove of DRB1*1454 (Figure 2B), matching the HLA-DRB type of LA patient 1. WIKI Pathway, KEGG Pathway, and Gene Ontology cellular localization analyses were used to further characterize source proteins of identified HLA-DR peptides (Figure 2C). Peptides from our TD dataset were enriched for proteins involved in ECM interactions, including focal adhesion, ECM–receptor interactions, transforming growth factor beta receptor signaling, and CCL18 signaling, which is induced by collagen and fibronectin produced by FLS.⁴² Furthermore, source proteins included 4 ECM, 11 secreted, 16 membrane-associated, and 21 cytosolic proteins (Figure 2C).

Among the self-peptides identified by both FV and TD analysis were two derived from LA autoantigens fibronectin (FN1) and ECGF (Table 1). The FN1 peptide identified, FN1_{1996–2010}, is predicted to bind to *0701, and the ECGF peptide, ECGF_{457–467}, is predicted to bind to *1454. Interestingly, both the FN1_{1996–2010} and the ECGF_{457–467} epitopes from our screening are identical or nearly identical to HLA-DR-bound peptides previously isolated from postinfectious LA synovial tissue³⁹ and match several epitopes from the Immune Epitope Database. Notably, the FN1_{1996–2010} peptide we identified is nearly identical to an autoreactive CD4+ T cell epitope in a subset of patients with postinfectious LA,¹ demonstrating that FLS are able to present Lyme autoantigens.

MHC-II expressed by IFN γ -stimulated murine FLS. In C3H/HeJ and C57BL/6 mice infected with *B. burgdorferi*, FLS are major sources of arthritogenic cytokines and chemokines in

inflamed joints.^{33,43} Furthermore, *B. burgdorferi* PG, which persists in joints of LA patients for months to several years following antibiotic therapy, is arthritogenic in BALB/c mice.²⁴ We hypothesized that in postinfectious LA, IFN γ produced by dysregulated T cells and persistent *B. burgdorferi* PG may induce FLS into an antigen presenting cell phenotype, driving CD4+ T cell activation in synovial tissue even after the infection itself is resolved using antibiotic therapy.²

Consistent with similar studies using primary human LA FLS,⁵ stimulation of C57BL/6 FLS with IFN γ (20 ng/mL) induced up-regulation of MHC-II I-ab approximately 1.5-fold after short-term stimulation (18 hours), and approximately two-fold after long-term stimulation (72 hours) with IFN γ . In comparison, long-term stimulation with both IFN γ and *B burgdorferi* PG (10 μ g/mL) significantly induced up-regulation of I-ab approximately 2.5-fold (Supplemental Figure S1A). MHC-II I-ab expression in IFN γ -stimulated BMDM was also significantly increased approximately five-fold at 72 hours after stimulation, but PG did not affect I-ab expression. Expression of FLS activation marker intercellular adhesion molecule 1 (ICAM-1), which is important for T cell attachment to antigen presenting cells (APCs) during antigen presentation and formation of immune synapses, was also up-regulated in FLS stimulated with IFN γ or IFN γ + PG for 24 hours, but not PG alone (Supplemental Figure S1B). This confirms that IFN γ , but not PG, is required for immune activation of FLS.

MHC-II expression is regulated by the IFN γ -induced transcriptional co-activator MHC-II transactivator (CIITA).⁴⁴ To determine whether IFN γ induces MHC-II expression in FLS in an endogenous, CIITA-dependent manner, FLS from CIITA-GFP-reporter mice were stimulated with IFN γ at various concentrations. FLS from CIITA-GFP-reporter mice had significantly increased fluorescence over controls, particularly when stimulated with 20 ng/mL IFN γ for 72 to 96 hours (Supplemental Figure S1C).

When stimulated with IFN γ , FLS also up-regulated production of IL-6, CCL2, and tumor necrosis factor alpha (TNF α), approximately two-fold compared to unstimulated controls and stimulation with *B burgdorferi* PG alone (Supplemental Figure S1D and E). Interestingly, stimulation with both IFN γ and *B burgdorferi* PG dampened production of IL-6 in FLS, compared to IFN γ alone, but both stimuli were required for BMDM up-regulation of IL-6. Stimulation with *B burgdorferi* PG alone did not affect the production of CCL2 or TNF α in FLS or BMDM.

Activation of CD4+ T cells by murine MHC-II+ FLS in an antigen-dependent manner. To evaluate whether MHC-II+ FLS can activate CD4+ T cells, we conducted a T cell proliferation assay using activated MHC-II+ FLS co-cultured with CD4+ T cells from mice that express a transgenic T cell receptor (TCR) specific for chicken OVA MHC-II antigen OVA_{323–339} as a model system to study antigen-specific CD4+ T cell responses (OT-II mouse model). OT-II T cells were co-cultured with FLS stimulated

Table 1. HLA-DR-presented peptides derived from LA autoantigens isolated from LA FLS*

Protein	Sequence	Source	Predicted HLA-DR binding (NetMHCIIpan4.0)
FN1	¹⁹⁹⁶ APS ¹⁹⁹⁶ NLR <u>FLATT</u> PNSL ²⁰¹⁰	This study	HLA-DRB1*0101, *0102, *0103, *0401, *0403, *0404, *0405, *0408, *0701 , *0803, *0901, *1001, *1601, DRB3*0202
FN1	¹⁹⁹⁶ APS ¹⁹⁹⁶ NLRFLATT <u>PNSL</u> ²⁰¹⁰	Wang et al, 2017	
FN1	¹⁹⁹⁶ APS ¹⁹⁹⁶ NLRFLATT <u>PNSLLVSW</u> ²⁰¹⁴	Kanjana et al, 2023	
FN1	¹⁹⁹⁶ APS ¹⁹⁹⁶ NLRFLATT <u>PNSL</u> ²⁰¹⁰	IEDB (ID 144206)	
ECGF	⁴⁵⁷ EAL <u>VLSDRAPF</u> ⁴⁶⁷	This study	HLA-DRB1*0301, *0305, *1104, *1301, *1302, *1303, *1401, *1402, *1454
ECGF	⁴⁶² SDRAPFA <u>APSPFAE</u> ⁴⁷⁵	Wang et al, 2017	
ECGF	⁴⁵⁵ LQEAL <u>VLSDRAPF</u> ⁴⁶⁷	IEDB (ID 1253447)	
ECGF	⁴⁵⁸ AL <u>VLSDRAPFA</u> APSPFAE ⁴⁶⁷	IEDB (ID 758118)	

*Superscripts indicate position of the peptide in the parent protein sequence. Underlined amino acids indicate the sequence corresponding to the HLA-DR binding groove. Bold numbers indicate predicted HLA-DR binding alleles corresponding to the HLA type of LA patient 1. IEDB epitope ID numbers were retrieved from iedb.org. FLS, fibroblast-like synoviocytes; FN1, fibronectin-1; ECGF, endothelial cell growth factor; IEDB, Immune Epitope Database; LA, Lyme arthritis.

with IFN γ , IFN γ + PG, or media alone (unstimulated FLS) in media containing the OVA peptide antigen. After five days, FLS and T cells were isolated, barcoded using split pool barcoding (Parse Biosciences), and gene expression was analyzed by single-cell (sc)RNA-seq (Figure 3A).

Initial uniform manifold approximation and projection (UMAP) of the mixed cell populations showed that FLS and CD4+ T cells formed distinct clusters. The FLS cluster was identified by high expression of genes encoding ECM proteins (eg, Col4a1) and fibroblast-specific growth factors (eg, Fgf2) (Figure 3B). CD4+ T cells were identified based on expression of the T cell marker CD3g and the Th cell marker Cd4 (Figure 3B).

FLS and CD4+ T cells were further analyzed by re-clustering (Figure 3C and D). FLS clustered into two subsets, an Il-6-high cluster that expressed high levels of inflammatory mediators such as Il6, Cxcl9, and Ccl2, and an Il-6 low cluster that did not express these inflammatory genes (Figure 3C). Notably, module scores for MHC-II Antigen Presentation (MHC-II AP) and MHC pathway showed that the Il6-high cluster had a pronounced MHC-II antigen presenting signature, consistent with phenotyping data shown in Supplemental Figure S1. Re-clustering of CD4+ T cells showed three distinct populations (Figure 3D). Cluster 1 expressed high levels of the proliferation marker Mki67 and T cell activation markers Il2ra and Cd44, whereas cluster 2 expressed low levels of these proliferation and activation genes. A third cluster, cluster 3, expressed intermediate levels of these markers. T helper module score showed that all three clusters had a T helper phenotype, but cluster 1 had the strongest proliferating Th1 phenotype, compared with clusters 2 and 3. Importantly, T cells from cluster 1 were only present in samples co-cultured with FLS preactivated with IFN γ or IFN γ + PG.

To validate the scRNA-seq data, the co-culture experiment was repeated and CD4+ OT-II T cell were analyzed for cell proliferation and cytokine secretion (Figure 4). Co-culture of OT-II CD4+ T cells with FLS primed with IFN γ and with the OT-II-OVA₃₂₃₋₃₃₉ epitope had approximately 25% increased levels of

CD4+ T cell proliferation, compared to approximately 15% seen using unstimulated FLS (Figure 4A). However, FLS primed with both IFN γ and *B burgdorferi* PG induced significantly increased (approximately 37%) levels of CD4+ T cell proliferation, compared with the other two conditions. T cells co-cultured with IFN γ -primed FLS given the OVA₂₅₇₋₂₆₄ control peptide, an alternative MHC-II binding epitope not recognized by the OT-II transgenic TCR, failed to induce T cell proliferation under any conditions, indicating that T cell proliferation was MHC-II epitope-dependent, and supports the scRNA-seq data (Figure 3D).

Priming of activated MHC-II+ FLS with PG had a pronounced adjuvant effect on the ability of FLS to induce multiple rounds of T cell proliferation. An average of 30.6% of CD4+ T cells underwent two or more rounds of proliferation when co-cultured with IFN γ + PG-activated MHC-II+ FLS compared to a significantly lower average of 17.3% of CD4+ T cells that underwent two or more rounds of proliferation when co-cultured with IFN γ -activated MHC-II+ FLS without PG (Figure 4A). Similar results were observed when full-length OVA was added to the co-culture medium (Figure 4B), indicating that FLS can take up, process, and load MHC-II antigen.

To characterize the CD4+ T cell responses induced by activated MHC-II+ FLS, we measured cytokines in supernatants collected from FLS-T cell co-culture experiments using the OT-II OVA₃₂₃₋₃₃₉ epitope as antigen (Figure 4C). Supernatants from T cells co-cultured with FLS primed with IFN γ alone had an average of 15.4 pg/mL of IL-10, which was significantly higher than unstimulated FLS (6.4 pg/mL), or FLS primed with IFN γ + PG (6.2 pg/mL). In contrast, supernatants from T cells co-cultured with FLS primed with both IFN γ and PG had elevated levels of IFN γ (369.5 pg/mL) compared with unprimed FLS (69.2 pg/mL) or FLS primed with IFN γ alone (143.1 pg/mL). As a result, the IFN γ :IL-10 ratio was approximately 10-fold higher in supernatants from T cells co-cultured with FLS primed with IFN γ + PG compared with the other two groups, indicating a skew toward a Th1 effector phenotype, consistent with the scRNA-seq data

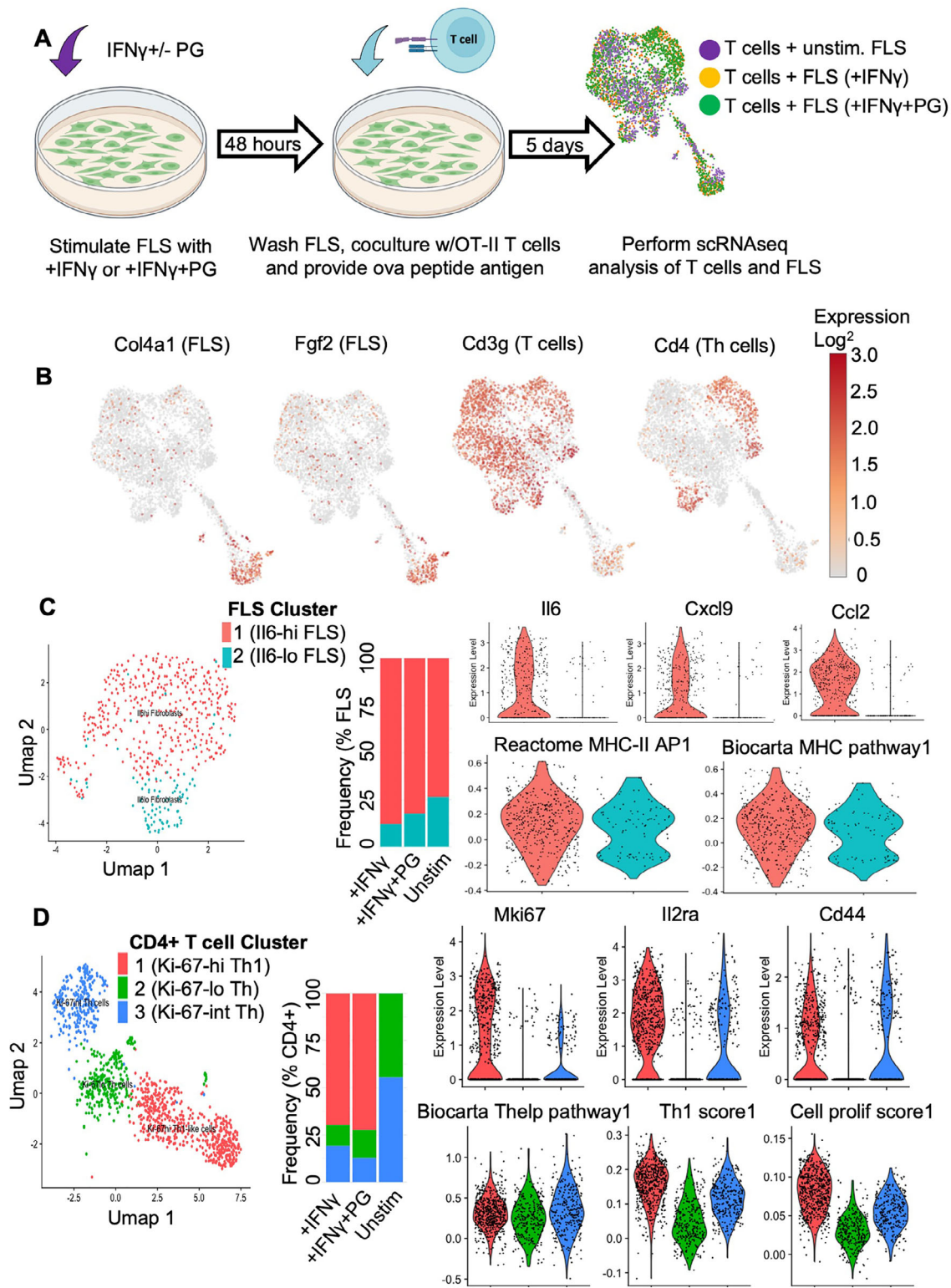


Figure 3. Stimulated mouse MHC-II+ FLS have an APC expression profile by scRNA-seq. (A) Primary mouse FLS were stimulated with media alone, IFN γ , or IFN γ + *B burgdorferi* PG for 48 hours and washed before isolation and co-culture of OT-II mouse T cells for five days and subsequent analysis by scRNA-seq. (B) UMAP showing FLS and CD4+ Th cell clusters. Reclustered UMAP and frequency plots showing (C) FLS and (D) CD4+ Th cells. Expression of I16, Cxcl9, and Ccl2 are shown to validate FLS clusters; and Mki67, Ii2ra, and Cd44 are shown to validate Th clusters. Thelper, Th1, and cell proliferation module scores were assessed in the CD4+ T cell clusters. APC, antigen presenting cell; FLS, fibroblast-like synoviocytes; IFN γ , interferon gamma; MHC-II, major histocompatibility complex class II; PG, peptidoglycan; scRNA-seq, single-cell RNA sequencing; UMAP, uniform manifold approximation and projection; unstim., unstimulated.

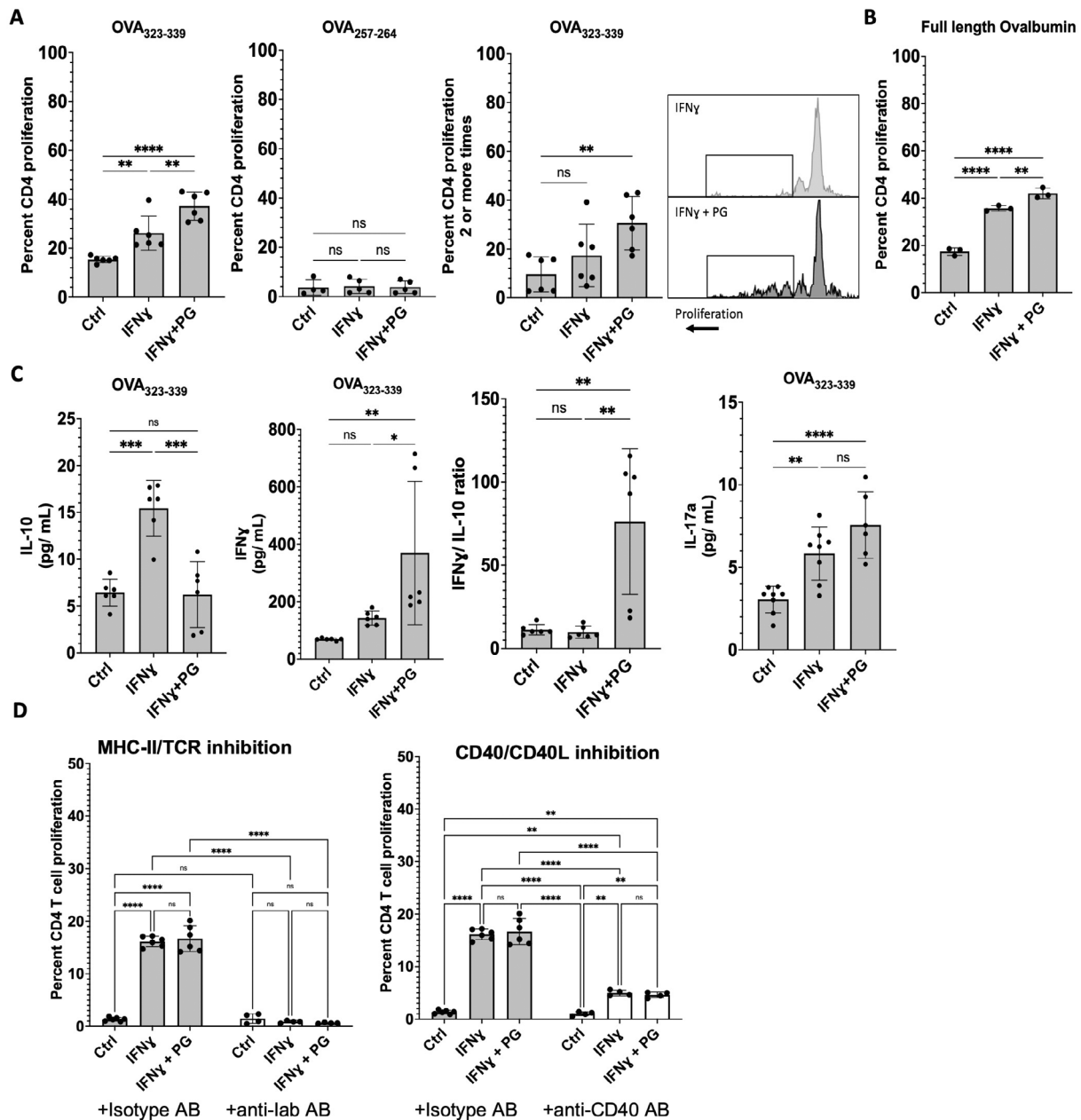


Figure 4. Stimulated mouse FLS elicit CD4⁺ T cell proliferation and is dependent on CD40-CD40L interaction. MHC-II⁺ FLS were induced with either IFN γ alone or IFN γ and *B burgdorferi* PG for 48 hours and washed before isolation and co-culture of OT-II mouse T cells for five days and subsequent analysis by flow cytometry. (A) Percentage of proliferating CD4⁺ T cells and cells that completed two or more rounds of replication, induced by MHC-II⁺ FLS when loaded with OVA peptides. (B) Percentage of proliferating CD4⁺ T cells induced by MHC-II⁺ FLS when loaded with full-length ovalbumin. (C) Co-culture cytokine analysis of IFN γ , IL-10, and IL-17a production. (D) CD4⁺ T cell proliferation was reduced upon inhibition of MHC-II/TCR and CD40/CD40L interactions using an anti-lab or anti-CD40 antibody, respectively, compared with isotype controls. Data from panels A and C were pooled from two independent experiments with three technical replicates. Data from panels B and D were from one experiment with three to six technical replicates for each group. Statistical analysis was performed using Tukey's multiple comparisons test, with a significance cutoff of $P < 0.05$. Error bars represent SD. Ctrl, control; FLS, fibroblast-like synoviocytes; IFN γ , interferon gamma; IL, interleukin; MHC-II, major histocompatibility complex class II; ns, not significant; OVA, ovalbumin; PG, peptidoglycan; TCR, T cell receptor.

(Figure 3D). FLS primed with either IFN γ or IFN γ + PG induced production of similarly elevated levels of IL-17A in supernatants of co-culture experiments compared with unprimed FLS (Figure 4C), suggesting that the addition of PG to FLS did not enhance IL-17 production.

Proliferation of CD4⁺ T cells was dependent on MHC-II/TCR and CD40/CD40L interactions. When anti-l-ab antibody was added to the co-culture, CD4⁺ T cell proliferation was completely ablated, compared with addition of an isotype control antibody (Figure 4D). Addition of a CD40-blocking antibody reduced

CD4+ T cell proliferation by approximately 75% compared with isotype antibody control (Figure 4D). Taken together, these data demonstrate that FLS stimulated with IFN γ can elicit activation and proliferation of CD4+ T cells in an antigen-dependent manner that is fully dependent on both MHC-II and mostly dependent on CD40, and T cell activation is enhanced with the addition of *B burgdorferi* PG.

DISCUSSION

This study shows that activated MHC-II+ FLS can process and present MHC-II antigens, including antigens associated with LA autoimmunity. Furthermore, we showed by scRNA-seq, by flow cytometry, and by functional assays that activated FLS can induce naive CD4+ T cell activation in an antigen- and CD40-dependent manner, particularly when primed with PG and IFN γ . These in vitro conditions partially recapitulate elements of the inflammatory microenvironment within the postinfectious LA synovial lesion.

These data also present mechanistic support of our earlier human studies by Kanjana et al¹ and Lochhead et al^{2,5} that strongly implicated MHC-II+ FLS as major contributors of Lyme autoantigens within the postinfectious LA inflammatory lesion. We propose that under pathogenic conditions, localized IFN γ responses during *B burgdorferi* infection stimulate FLS into an activated MHC-II+ immune effector phenotype. If IFN γ levels within the joint microenvironment become excessive due to autoimmunity and/or accumulation of *B burgdorferi* PG, activated MHC-II+ FLS can prolong pathogenic T cell reactivity, perpetuating tissue-localized inflammation even in the absence of active infection.

We report that IFN γ induces murine FLS to up-regulate numerous genes involved in uptake, processing, and presentation of MHC-II antigen. By using an immunopeptidomics approach, we characterized peptides presented by human LA MHC-II+ FLS and found that these cells are able to present peptides derived from LA autoantigen FN1, which raises the possibility that these activated MHC-II+ FLS may drive ECM autoimmunity following *B burgdorferi* infection. We also showed that the adjuvant effects of *B burgdorferi* PG can fundamentally alter T cell responses induced by MHC-II+ FLS. We show that MHC-II+ FLS, induced by IFN γ , can take up antigen from the environment and induce T cell activation in an antigen-dependent manner, which is exacerbated by *B burgdorferi* PG to a robust Th1-like response. Yet, in the absence of PG, T cell proliferation is attenuated and is accompanied by elevated production of the immunomodulatory cytokine IL-10. Overall, these findings support observations in previous studies of postinfectious LA,^{5,24,45} validating our in vitro model of LA. Together, these data show that activated MHC-II+ FLS function as inducible APCs to promote ongoing recruitment and activation of IFN γ -producing lymphocytes.

Other studies from our group have demonstrated that tissue-localized antigen presentation in the joint is fundamental for driving T cell-mediated autoimmune inflammation against self-peptides derived from proteins at sites of infection associated with synovial tissue damage.^{1,19–22} Identification of FN1 as an FLS-presented peptide was particularly noteworthy, because autoreactive CD4+ T cells targeting FN1 and other FLS-derived ECM proteins have a marked Th1 phenotype and are detected in over 50% of patients with postinfectious LA.¹ Our study suggests that retained *B burgdorferi* PG plays a critical role in perpetuating Th1 reactivity against autoreactive ECM proteins in postinfectious LA.²⁴

Our data indicate that activated MHC-II+ FLS phenotypes are plastic and can be dramatically altered by presence or absence of PG. This finding may have broad implication in other chronic inflammatory joint diseases, particularly when an infection is suspected as an autoimmune trigger. For example, previous reports have identified PG in inflamed synovia from patients with RA⁴⁶ and from patients undergoing total knee arthroplasty.²⁶ This idea merits a re-examination of the role of PG and other PAMPs in RA autoimmunity.

Our study also has potential clinical and therapeutic implications. A recent study showed that part of the therapeutic effect of JAK inhibitors is reversing the proinflammatory effects of activated MHC-II+ FLS by interfering with IFN γ signaling.¹¹ We and others³⁸ have shown that FLS lack expression of canonical CD80 and CD86 co-stimulatory molecules. As shown in this and other studies, FLS express an altered repertoire of co-stimulatory molecules, including CD40.^{38,47} Additionally, CD40/CD40L is a promising therapeutic target in both autoimmunity⁴⁸ and cancer,⁴⁹ in part due to targeting CD40 expression by fibroblasts. Synovial fibroblast expression of CD40 promotes T cell activation in RA,⁵⁰ and fibroblast-targeted CD40 activation leads to solid tumor eradication.⁵¹

There are some limitations with our study. Although we were able to isolate HLA-DR+ FLS-presented peptides from one patient after in vitro stimulation, we are unable to obtain sufficient numbers of FLS directly from patients' tissue to determine what peptides are presented by FLS ex vivo. No mouse models of Lyme autoimmunity exist, and no mouse-specific autoimmune T cell epitopes have been identified. The lack of a suitable mouse model was the rationale for using the model OT-II system. Thus, novel mouse models of autoimmunity in LA, likely targeting FN1, must be developed in order to validate these findings using in vivo models. Another limitation of this study is that, although we showed that CD40 expression by fibroblasts is required for full activation of CD4+ T cells, other co-stimulatory molecules and/or immune checkpoints are likely involved in regulation of T cell–fibroblast interactions, and T cell-activating signals downstream of CD40 remain incompletely understood.

In conclusion, this study demonstrates that activated MHC-II+ FLS can present HLA-DR-presented Lyme autoantigens and

are inducible APCs that acquire a potent T cell-activating phenotype, particularly when exposed to IFN γ and PG. These findings add to a growing body of evidence that MHC-II+ stromal cells play critical roles in shaping tissue-localized CD4+ T cell responses in a wide variety of diseases such as RA,^{10,52} cancer,⁵³ and cardiovascular disease.⁵⁴

ACKNOWLEDGMENTS

We extend our sincerest gratitude to Catherine Costello, PhD, for her invaluable assistance with the immunopeptidomics study. We would also like to acknowledge Mark Wooten, PhD, for providing the CIITA EGFP-reporter mouse and for reviewing the manuscript; Savannah Neu at the Versiti Flow Cytometry Core for flow cytometry assistance; John Corbett, PhD, Director of the MCW Center for Biomedical Mass Spectrometry Research for providing us with mass spectrometry resources and expertise; and Michael Dwinell, PhD, Director of the MCW Center for Immunology for providing equipment and scientific resources. We would also like to thank Jenifer Coburn, PhD, for generously providing the *B burgdorferi* strains used in this study.

AUTHOR CONTRIBUTIONS

All authors contributed to at least one of the following manuscript preparation roles: conceptualization AND/OR methodology, software, investigation, formal analysis, data curation, visualization, and validation AND drafting or reviewing/editing the final draft. As corresponding author, Dr Lochhead confirms that all authors have provided the final approval of the version to be published, and takes responsibility for the affirmations regarding article submission (eg, not under consideration by another journal), the integrity of the data presented, and the statements regarding compliance with institutional review board/Helsinki Declaration requirements.

DATA AVAILABILITY STATEMENT

The data that support the findings of this study are available from the corresponding author upon reasonable request.

REFERENCES

- Kanjana K, Strle K, Lochhead RB, et al. Autoimmunity to synovial extracellular matrix proteins in patients with postinfectious Lyme arthritis. *J Clin Invest* 2023;133(17):e161170.
- Lochhead RB, Strle K, Arvikar SL, et al. Lyme arthritis: linking infection, inflammation and autoimmunity. *Nat Rev Rheumatol* 2021;17(8):449–461.
- Nygaard G, Firestein GS. Restoring synovial homeostasis in rheumatoid arthritis by targeting fibroblast-like synoviocytes. *Nat Rev Rheumatol* 2020;16(6):316–333.
- Wei K, Nguyen HN, Brenner MB. Fibroblast pathology in inflammatory diseases. *J Clin Invest* 2021;131(20):e149538.
- Lochhead RB, Ordoñez D, Arvikar SL, et al. Interferon-gamma production in Lyme arthritis synovial tissue promotes differentiation of fibroblast-like synoviocytes into immune effector cells. *Cell Microbiol* 2019;21(2):e12992.
- Plikus MV, Wang X, Sinha S, et al. Fibroblasts: origins, definitions, and functions in health and disease. *Cell* 2021;184(15):3852–3872.
- Carmona-Rivera C, Carlucci PM, Moore E, et al. Synovial fibroblast-neutrophil interactions promote pathogenic adaptive immunity in rheumatoid arthritis. *Sci Immunol* 2017;2(10):eaag3358.
- Croft AP, Campos J, Jansen K, et al. Distinct fibroblast subsets drive inflammation and damage in arthritis. *Nature* 2019;570(7760):246–251.
- Mizoguchi F, Slowikowski K, Wei K, et al. Functionally distinct disease-associated fibroblast subsets in rheumatoid arthritis. *Nat Commun* 2018;9(1):789.
- Tran CN, Davis MJ, Tesmer LA, et al. Presentation of arthritogenic peptide to antigen-specific T cells by fibroblast-like synoviocytes. *Arthritis Rheum* 2007;56(5):1497–1506.
- Zhao S, Grieshaber-Bouyer R, Rao DA, et al. Effect of JAK inhibition on the induction of proinflammatory HLA-DR+CD90+ rheumatoid arthritis synovial fibroblasts by interferon- γ . *Arthritis Rheumatol* 2022;74(3):441–452.
- Alivernini S, MacDonald L, Elmesmari A, et al. Distinct synovial tissue macrophage subsets regulate inflammation and remission in rheumatoid arthritis. *Nat Med* 2020;26(8):1295–1306.
- Dong Y, Zhou G, Cao W, et al. Global seroprevalence and socio-demographic characteristics of *Borrelia burgdorferi sensu lato* in human populations: a systematic review and meta-analysis. *BMJ Glob Health* 2022;7(6):e007744.
- Kugeler KJ, Schwartz AM, Delorey MJ, et al. Estimating the frequency of Lyme disease diagnoses, United States, 2010–2018. *Emerg Infect Dis* 2021;27(2):616–619.
- Arvikar SL, Steere AC. Lyme arthritis. *Infect Dis Clin North Am* 2022;36(3):563–577.
- Snydman DR, Schenkein DP, Berardi VP, et al. *Borrelia burgdorferi* in joint fluid in chronic Lyme arthritis. *Ann Intern Med* 1986;104(6):798–800.
- Steere AC. Lyme disease. *N Engl J Med* 1989;321(9):586–596.
- Steere AC, Schoen RT, Taylor E. The clinical evolution of Lyme arthritis. *Ann Intern Med* 1987;107(5):725–731.
- Crowley JT, Drouin EE, Pianta A, et al. A highly expressed human protein, apolipoprotein B-100, serves as an autoantigen in a subgroup of patients with Lyme disease. *J Infect Dis* 2015;212(11):1841–1850.
- Crowley JT, Strle K, Drouin EE, et al. Matrix metalloproteinase-10 is a target of T and B cell responses that correlate with synovial pathology in patients with antibiotic-refractory Lyme arthritis. *J Autoimmun* 2016;69:24–37.
- Drouin EE, Seward RJ, Strle K, et al. A novel human autoantigen, endothelial cell growth factor, is a target of T and B cell responses in patients with Lyme disease. *Arthritis Rheum* 2013;65(1):186–196.
- Pianta A, Drouin EE, Crowley JT, et al. Annexin A2 is a target of auto-immune T and B cell responses associated with synovial fibroblast proliferation in patients with antibiotic-refractory Lyme arthritis. *Clin Immunol* 2015;160(2):336–341.
- Bockenstedt LK, Gonzalez DG, Haberman AM, et al. Spirochete antigens persist near cartilage after murine Lyme borreliosis therapy. *J Clin Invest* 2012;122(7):2652–2660.
- Jutras BL, Lochhead RB, Kloos ZA, et al. *Borrelia burgdorferi* peptidoglycan is a persistent antigen in patients with Lyme arthritis. *Proc Natl Acad Sci USA* 2019;116(27):13498–13507.
- Schrijver IA, Melief MJ, Markusse HM, et al. Peptidoglycan from sterile human spleen induces T-cell proliferation and inflammatory mediators in rheumatoid arthritis patients and healthy subjects. *Rheumatology (Oxford)* 2001;40(4):438–446.
- Holub MN, Wahhab A, Rouse JR, et al. Peptidoglycan in osteoarthritis synovial tissue is associated with joint inflammation. *Res Sq Preprint* posted online April 28, 2023. doi: [10.21203/rs.3.rs-2842385/v1](https://doi.org/10.21203/rs.3.rs-2842385/v1)
- Chiu YC, Lin CY, Chen CP, et al. Peptidoglycan enhances IL-6 production in human synovial fibroblasts via TLR2 receptor, focal

- adhesion kinase, Akt, and AP-1- dependent pathway. *J Immunol* 2009;183(4):2785–2792.
28. Kyburz D, Rethage J, Seibl R, et al. Bacterial peptidoglycans but not CpG oligodeoxynucleotides activate synovial fibroblasts by toll-like receptor signaling. *Arthritis Rheum* 2003;48(3):642–650.
 29. Centers for Disease Control and Prevention (CDC). Recommendations for test performance and interpretation from the Second National Conference on Serologic Diagnosis of Lyme Disease. *MMWR Morb Mortal Wkly Rep* 1995;44(31):590–591.
 30. Lantos PM, Rumbaugh J, Bockenstedt LK, et al. Clinical practice guidelines by the Infectious Diseases Society of America (IDSA), American Academy of Neurology (AAN), and American College of Rheumatology (ACR): 2020 guidelines for the prevention, diagnosis and treatment of Lyme disease. *Clin Infect Dis* 2021;72(1):1–8.
 31. Seward RJ, Drouin EE, Steere AC, et al. Peptides presented by HLA-DR molecules in synovia of patients with rheumatoid arthritis or antibiotic-refractory Lyme arthritis. *Mol Cell Proteomics* 2011;10(3):M1110.002477.
 32. Boes M, Cerny J, Massol R, et al. T-cell engagement of dendritic cells rapidly rearranges MHC class II transport. *Nature* 2002;418(6901):983–938.
 33. Lochhead RB, Sonderegger FL, Ma Y, et al. Endothelial cells and fibroblasts amplify the arthritogenic type I IFN response in murine Lyme disease and are major sources of chemokines in *Borrelia burgdorferi*-infected joint tissue. *J Immunol* 2012;189(5):2488–2501.
 34. Davis MM, Brock AM, DeHart TG, et al. The peptidoglycan-associated protein NapA plays an important role in the envelope integrity and in the pathogenesis of the Lyme disease spirochete. *PLoS Pathog* 2021;17(5):e1009546.
 35. Häupl T, Hahn G, Rittig M, et al. Persistence of *Borrelia burgdorferi* in ligamentous tissue from a patient with chronic Lyme borreliosis. *Arthritis Rheum* 1993;36(11):1621–1626.
 36. Steere AC. Musculoskeletal manifestations of Lyme disease. *Am J Med* 1995;98(4A):44S–48S; discussion 8S–51S.
 37. Miller JB, Albayda J, Aucott JN. The value of musculoskeletal ultrasound for evaluation of postinfectious Lyme arthritis. *J Clin Rheumatol* 2022;28(2):e605–e608.
 38. Tran CN, Thacker SG, Louie DM, et al. Interactions of T cells with fibroblast-like synoviocytes: role of the B7 family costimulatory ligand B7-H3. *J Immunol* 2008;180(5):2989–2998.
 39. Wang Q, Drouin EE, Yao C, et al. Immunogenic HLA-DR-presented self-peptides identified directly from clinical samples of synovial tissue, synovial fluid, or peripheral blood in patients with rheumatoid arthritis or Lyme arthritis. *J Proteome Res* 2017;16(1):122–136.
 40. Barbour AG, Jasinskas A, Kayala MA, et al. A genome-wide proteome array reveals a limited set of immunogens in natural infections of humans and white-footed mice with *Borrelia burgdorferi*. *Infect Immun* 2008;76(8):3374–3389.
 41. Pishesha N, Harmand TJ, Ploegh HL. A guide to antigen processing and presentation. *Nat Rev Immunol* 2022;22(12):751–764.
 42. Schraufstatter IU, Zhao M, Khaldoyanidi SK, et al. The chemokine CCL18 causes maturation of cultured monocytes to macrophages in the M2 spectrum. *Immunology* 2012;135(4):287–298.
 43. Helble JD, Walsh MJ, McCarthy JE, et al. Single-cell RNA sequencing of murine ankle joints over time reveals distinct transcriptional changes following *Borrelia burgdorferi* infection. *iScience* 2023;26(11):108217.
 44. Mach B, Steimle V, Martinez-Soria E, et al. Regulation of MHC class II genes: lessons from a disease. *Annu Rev Immunol* 1996;14:301–331.
 45. Lochhead RB, Arvikar SL, Aversa JM, et al. Robust interferon signature and suppressed tissue repair gene expression in synovial tissue from patients with postinfectious, *Borrelia burgdorferi*-induced Lyme arthritis. *Cell Microbiol* 2019;21(2):e12954.
 46. van der Heijden IM, Wilbrink B, Tchvetverikov I, et al. Presence of bacterial DNA and bacterial peptidoglycans in joints of patients with rheumatoid arthritis and other arthritides. *Arthritis Rheum* 2000;43(3):593–598.
 47. Sempowski GD, Chess PR, Phipps RP. CD40 is a functional activation antigen and B7-independent T cell costimulatory molecule on normal human lung fibroblasts. *J Immunol* 1997;158(10):4670–4677.
 48. Vermersch P, Granziera C, Mao-Draayer Y, et al. Frexalimab Phase 2 Trial Group. Inhibition of CD40L with frexalimab in multiple sclerosis. *N Engl J Med* 2024;390(7):589–600.
 49. Vonderheide RH. CD40 agonist antibodies in cancer immunotherapy. *Annu Rev Med* 2020;71:47–58.
 50. Kim KW, Cho ML, Kim HR, et al. Up-regulation of stromal cell-derived factor 1 (CXCL12) production in rheumatoid synovial fibroblasts through interactions with T lymphocytes: role of interleukin-17 and CD40L-CD40 interaction. *Arthritis Rheum* 2007;56(4):1076–1086.
 51. Rigamonti N, Veitonmäki N, Domke C, et al. A multispecific anti-CD40 DARPin construct induces tumor-selective CD40 activation and tumor regression. *Cancer Immunol Res* 2022;10(5):626–640.
 52. Carmona-Rivera C, Carlucci PM, Goel RR, et al. Neutrophil extracellular traps mediate articular cartilage damage and enhance cartilage component immunogenicity in rheumatoid arthritis. *JCI Insight* 2020;5(13):e139388.
 53. Huang H, Wang Z, Zhang Y, et al. Mesothelial cell-derived antigen-presenting cancer-associated fibroblasts induce expansion of regulatory T cells in pancreatic cancer. *Cancer Cell* 2022;40(6):656–673.e7.
 54. Ngwenyama N, Kaur K, Bugg D, et al. Antigen presentation by cardiac fibroblasts promotes cardiac dysfunction. *Nat Cardiovasc Res* 2022;1(8):761–774.